Ab-Initio Calculation of the Charge Topology of the Oxygen Active Site of the (001) Surface of Pure and Doped MgO

Yosslen Aray,* Felix Rosillo,† and Juan Murgich

Contribution from the Centro de Química, IVIC, Apartado 21827, Caracas 1020A, Venezuela

Received February 21, 1994[⊗]

Abstract: An *ab-initio* calculation of the charge density $\varrho(r)$ of the O site in the (001) surface of pure MgO and that doped with Li, Na, and K and with a Mg^{1+} vacancy is reported. An embedded cluster (Mg_4XO_5 with X = Mg, Mg^+ vacancy, Li^+, Na^+, and K^+) in a set of point charges that simulated the rest of the crystal was employed in the calculation. The results obtained with the embedded cluster methods for the O sites were shown to be within 2% of those calculated in slabs composed by one to three layers of pure MgO with an *ab-initio* method for periodic structures. The Laplacian of the charge density, $-\nabla^2\varrho(r)$, of the O valence shell obtained with both methods showed that, in pure and perfect MgO, the O^{2-} ion has a local maximum in $-\nabla\varrho(r)$ in a direction perpendicular to the (001) surface that does not favor the H abstraction from methane. It was also found with the embedded cluster method that doping with alkali metal ions and the Mg^+ vacancy formation produced important changes in the atomic graphs of the O ion present at the surface. These changes were such that the local minima in $\varrho(r)$ of the O valence shell were produced along the O–metal bond direction. These local minima provide the sites where the electron-rich C–H bond of methane is attracted and the H abstraction occurs. The more pronounced minimum corresponded to the Li doping, decreasing when passing to Na and K and when a Mg^+ vacancy was created below the O site. This trend reproduces the known reaction barriers and supports the relationship between the reactivity of the MgO surfaces and the characteristics of the topology of $\varrho(r)$ of the valence shell of the O^- ion.

Introduction

Alkali-doped metal oxides have been successfully employed in the synthesis of ethane and other higher hydrocarbons from natural gas.[1–3] Both pure MgO and MgO doped with Li, Na, and K are known as catalysts for methane transformation,[2,3] in presence of O_2. These catalysts are able to generate CH_3 free radicals which, in further reactions, produce ethane and other hydrocarbons.[2,3] In order to obtain information about this process, an *ab-initio* MO study of the charge topology of the active sites of the (001) surface of MgO has been performed.

The surfaces of MgO have been calculated by means of different methods using both *ab-initio* and semiempirical approaches.[4,5] Cluster and full crystal calculations have been performed on the bulk and on surfaces of pure and doped MgO.[4–7] These calculations were focused toward the energetics of the bulk or the surface and the H abstraction. These studies did not deal with the topology of the charge distribution of the active sites and its relationship with the chemical reactivity. Experimental results have shown that the concentration of O^- radical ions at the surface has a strong correlation with the catalytical properties of MgO.[8] Moreover, the enhanced reactivity of MgO when doped with Li, Na, and K was explained[9,10] by a net increase in the number of O^- sites in the surface. It is clear, then, that a more detailed study of the charge distribution of these sites will help in the understanding of the properties of MgO as a catalyst.

Recently, the F centers of the MgO surface were considered to be responsible for the methane activation instead of the O^- sites promoted by Li.[11] This claim was based on (a) the apparent parallel correlation found between the density of F defects and the ethane formation rate with respect to the sample pretreatment temperature and (b) the observation that the same activation energy was found for methane activation over pure and over Li-promoted MgO films. An analysis of the results shown in ref 11 indictates that the plot of high-resolution electron energy loss intensity (which is related to the density of F centers) vs temperature has only one portion that parallels the increase of the ethane formation rate. As the temperature is increased above 1200 K, the intensity reaches a maximum and then starts to *decrease* while the formation rate mantains a linear *increase* over this whole range. Clearly, this behavior is not consistent with the parallel correlation claimed in ref 11. The equality in the activation energy for methane activation over different MgO films was derived from the comparison of the slopes of two lines determined,[11] in one case by only three and in the other by five widely scattered points. Clearly, the error (20%) quoted for the activation energy is unrealistic in view of the scatter and the meager number of points employed in the analysis. Then, the claim about the equality of the activation energy is not sustainable by the data presented in ref 11. It is quite

† Departmento de Química, Facultad Experimental de Ciencias, Universidad del Zulia, Maracaibo, Venezuela.

⊗ Abstract published in *Advance ACS Abstracts*, September 15, 1994.

(1) (a) Pitchai, R.; Klier, K. *Catal. Rev. Sci. Eng.* **1986**, *28*, 13–88. (b) Lin, C. H.; Wang, J. X.; Lundsford, J. H. *J. Catal.* **1988**, *111*, 302–316. (c) Kooh, A.; Mimoun, H.; Cameron, C. J. *Catal. Today* **1989**, *4*, 333–344.

(2) (a) Agarwal, S. K.; Migone, R. A.; Marcelin, G. *J. Catal.* **1990**, *123*, 228–235. (b) Choudhary, V. R.; Rane, V. H.; Chaudhari, S. T. *Catal. Lett.* **1990**, *6*, 95–98.

(3) (a) Dai, G. H.; Yan, Q. J.; Wang, Y.; Liu, Q. S. *Chem. Phys.* **1991**, *155*, 275–284. (b) Bychkov, V. Y.; Sinev, M. Y.; Korchak, V. N.; Aptekar, E. L.; Krylov, O. V. *Kinet. Catal.* **1989**, *30*, 989–998. (c) Martin, G. A.; Bernal, S.; Perrichon, V.; Mirodatos, C. *Catal. Today* **1992**, *13*, 487–494.

(4) Børve, K. J.; Pettersson, L. G. M. *J. Phys. Chem.* **1991**, *95*, 3214–3217.

(5) Zivcovich-Wilson, C. M.; González-Luque, R.; Viruela-Martín, P. M. *J. Mol. Struct. (THEOCHEM)* **1990**, *208*, 153–162.

(6) Viruela-Martín, P. M.; Viruela-Martín, R.; Zicovich-Wilson, C. M.; Tomás-Vert, F. *J. Mol. Catal.* **1991**, *64*, 191–200.

(7) Zhidomirov, G. M.; Zhanpeisov, N. U. *Catal. Today* **1992**, *13*, 517–522.

(8) Driscoll, D. J.; Lunsford, J. H. *J. Phys. Chem.* **1985**, *89*, 4415.

(9) Lin, C. H.; Ito, T.; Wang, T. X.; Lunsford, J. H. *J. Am. Chem. Soc.* **1987**, *109*, 4808.

(10) (a) Børve, K. J.; Pettersson, L. G. M. *J. Phys. Chem.* **1991**, *95*, 7401–7405. (b) Børve, K. J. *J. Chem. Phys.* **1991**, *95*, 4626–4631.

(11) Chu, M. C.; Truong, C. M.; Coulter, K.; Goodman, D. W. *J. Catal.* **1993**, *140*, 344–352.

0002-7863/94/1516-10639$04.50/0

possible that the F centers may play a role in the activation of methane over MgO surfaces, but one has to wait until reliable data are obtained in order to establish the importance of their contribution. On the other hand, there is a large amount of sound experimental data supporting the importance of the O^- centers in the activation of methane over MgO surfaces. Consequently, it will be assumed that the O^- centers are one of the more important factors in the activation of methane in MgO surfaces.

Bader and co-workers[12] have shown that the reactivity of molecules is reflected in the topology of the Laplacian of the charge density, $\nabla^2\varrho(r)$. They found a correlation between the topology of $-\nabla^2\varrho(r)$ in the valence shells and the location of nucleophilic or electrophilic active sites in organic molecules. The Laplacian of $\varrho(r)$ reveals where electron density is locally concentrated ($\nabla^2\varrho < 0$) or depleted ($\nabla^2\varrho > 0$). In a Lewis acid and base, one has, in the valence shells, regions of local charge depletion and concentration, respectively.[12] Thus, in general, the reaction of a nucleophile with an electrophile corresponds to the interaction of a local center of charge concentration in one molecule with one of local depletion in another. The topological approach[12] has the advantage that the chemical reactivity is directly interpreted in terms of a physical observable, such as $\varrho(r)$, and not, for example, in terms of the energy levels of a particular set of molecular orbitals. Nucleophilic addition in double bonds,[13] electrophilic aromatic substitution,[14] and the S_N2 and S_E2 mechanisms[13] have been explained in terms of this theory. Recently,[15] an *ab-initio* MO study of the H abstraction from CH_4 by MgO and LiO molecules in the gas phase showed that the topology of the O valence shell charge distribution plays a determining role in this homolitic process. It was shown in ref 15 that the molecular states in which the O valence shell had a local minimum in its valence charge concentration along the Mg−O direction were highly reactive toward H abstraction from methane. This calculation was performed in the gas phase and showed that the theory developed by Bader and co-workers[12] for the heterolitic reactions (classical Lewis acid−base interactions) could be extended to homolitic ones such as the H abstraction from methane. In the present study, we have applied the theory of Bader and co-workers[12] to the study of the surfaces of solid MgO, both pure and doped, to determine whether the reactive topology of the O^- charge distribution, found for isolated MgO and LiO molecules, was also present at some O sites of its (001) surface.

As the atomic charge topology is very sensitive to the method employed in the calculation of the wave functions, a two-step approach was followed in the calculation of the (001) surface of MgO. In the first one, the bulk and several infinite slabs of various thickness that modeled the surface were calculated by means of the exact-exchange Hartree−Fock crystalline-orbital LCAO SCF CRYSTAL 92 program. The resulting charge topology was then compared with that obtained by means of the Gaussian 92 program, from a cluster of Mg and O atoms embedded in a set of point charges that simulated the rest of the MgO crystal. This comparison provided a critical check of the accuracy of the results obtained with the embedded cluster. If the cluster approach were successful, it would allow the study of doped and other more complex MgO systems. After finding an excellent match between the charge topologies obtained with these two methods in pure MgO, properly embedded clusters of Mg_4XO_5, with X = Mg, a Mg^+ vacancy, Li^+, Na^+, and K^+, were calculated using an *ab-initio* method. It was found that, in pure and perfect MgO, the O^{2-} ion of the (001) surface has a local maximum in the charge concentration in a direction perpendicular to it that does not favor the H abstraction from methane. It was also found that doping with alkali metals and the Mg^+ vacancy formation in the second layer produced strong changes in the atomic graphs of the O ion present at the surface. These changes were such that a local depletion in the charge concentration of the O valence shell was produced along the O−X bond directions. The more pronounced minimum corresponded to the Li doping, decreasing for Na and K and when a Mg^+ vacancy was created in the second layer. This trend reproduces the known reaction barriers and supports the relationship between the reactivity of the MgO surfaces and the topology of the valence shell charge distribution of the O^- ion.

Computational Details

The Hartree−Fock crystalline-orbital LCAO SCF CRYSTAL 92 program[16] was used in the calculation of bulk and slabs of MgO. This program has been employed before in the calculation of bulk and surfaces of MgO[17-19] in bulk Li_2O and other ionic solids.[20] In MgO, it was found that only a very slight rumpling (less than 2%) was present at the (001) surface of MgO[17] so that the surface relaxation effects on the charge distribution are expected to be small.

The most stable phase of MgO is cubic and has the *Fm3m* space group with $a = 4.210$ Å.[18] The lack of translational symmetry in the direction orthogonal to the surface of MgO can be dealt with by approximating the semi-infinite crystal by a finite slab.[17] In order to determine the most convenient model, we have considered slabs formed with one, two, and three atomic planes perpendicular to the (001) direction of MgO.

The choice of the basis set is extremely important both in terms of accuracy of the charge density obtained and the computer time required for its calculation.[20] In this work, the high-quality basis set employed in the previous calculation of MgO was used,[17] while for the Li and Na salts, the sets employed were the same as in ref 20. The extended set for the MgO calculation contains nine independent functions (three s and six p) for each atom. The two inner shells of the O atom were optimized in the isolated atom while the exponent of the more external sp function was optimized in the bulk.[18] The 1s and 2sp Mg functions employed in the calculation represent a variationally optimized solution for the isolated Mg^{2+} ion. Additionally, a 3sp function was used in order to allow for nontotally ionic solutions.[18]

The CRYSTAL code provides information only about periodic systems formed with electronic shells with spin multiplicity equal to 1.[16] Then, the effect of isolated doping or the presence of a finite number of vacancies cannot be studied with this program. For this reason, small atomic clusters of MgO were employed in order to study these effects on the charge distribution. A cluster formed by Mg_4XO_5 atoms (with X = Mg, Li^+, Na^+, K^+, and a Mg^+ vacancy), shown in Figure 1, was employed in the present calculation. The doping ion or

(12) (a) Bader, R. F. W. *Atoms in Molecules: a Quantum Theory*; Clarendon: Oxford, U.K., 1990; Chapter 7. (b) Bader, R. F. W.; Essén, H. *J. Chem. Phys.* **1984**, *80*, 1943−1960. (c) Bader, R. F. W.; MacDougall, P. J.; Lau, C. D. H. *J. Am. Chem. Soc.* **1984**, *106*, 1594−1605. (d) Bader, R. F. W.; MacDougall, P. J. *J. Am. Chem. Soc.* **1985**, *107*, 6788−6795. (e) Bader, R. F. W.; Popelier, P. L. A.; Chang, C. *J. Mol. Struct. (THEOCHEM)* **1992**, *255*, 145−171.

(13) Carrol, M. T.; Cheeseman, J. R.; Osman, R.; Weinstein, H. *J. Phys. Chem.* **1989**, *93*, 5120−5123.

(14) Bader, R. F. W.; Chang, C. *J. Phys. Chem.* **1989**, *93*, 2946−2956.

(15) Aray, Y.; Rodríguez, J.; Murgich, J.; Ruette, F. *J. Phys. Chem.* **1993**, *97*, 8393−8398.

(16) Dovesi, R.; Saunders, V. R.; Roetti, C. *CRYSTAL 92*; Theoretical Chemistry Group: University of Turin, Italy, and SERC, Daresbury Laboratory, U.K., 1992.

(17) Causà, M.; Dovesi, R.; Kotomin, E.; Pisani, C. *J. Phys. C: Solid State Phys.* **1987**, *20*, 4983−4990.

(18) Causà, M.; Dovesi, R.; Pisani, C.; Roetti, C. *Phys. Rev.* **1986**, *B33*, 1308−1316.

(19) Causà, M.; Dovesi, R.; Pisani, C.; Roetti, C. *Surf. Sci.* **1986**, *175*, 551−560.

(20) Dovesi, R.; Roetti, C.; Freyria-Fava, C.; Prencipe, M. *Chem. Phys.* **1991**, *156*, 11−19.

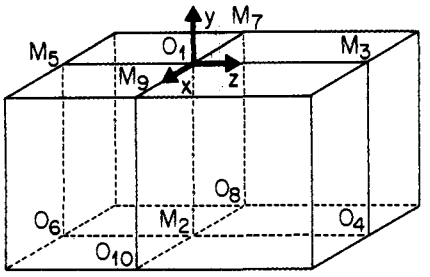

Figure 1. Geometry of the Mg_5O_5 cluster model of the MgO (001) plane. M_i indicates the position occupied by the *i*th Mg atom. All the calculations of the topology of $-\nabla^2\varrho(r)$ were made on the O site of this cluster.

the vacancy was located in the second layer of the crystal. The cluster was embedded in a set of point charges by means of the Embedded Cluster Methodology (ECM) available as a part of the Gaussian 92 program.[21] The ECM describes the crystalline system by means of a combination of quantum and molecular mechanical tools. It performs a coupling of the quantum mechanical description of the cluster with a molecular mechanical description of the surrounding structure of the crystal. In the present case, the parts of the crystal outside the cluster are modeled by a set of regularly spaced ±2 point charges. The molecular mechanical Hamiltonian contains a description of the Coulomb interactions and, by addition to the quantum mechanical Hamiltonian, accounts for the polarization of the electron distribution of the cluster in the presence of the electrostatic potential of the rest of the crystal.[22] The size of the cluster is similar to that used by Bøorve and Pettersson in their CI calculation[10a] and provides a reasonable compromise between hardware requirements and accuracy obtained in the charge distribution.

When a dopant was introduced in the MgO cluster, the lattice relaxation that resulted from the Mg substitution was modeled by manually introducing variations in the Mg−O distances until a minimum in the total energy was obtained.

The topology of $-\nabla^2\varrho(r)$ was analyzed by means of the Bader's formalism[12] using the Bubble program of the new AIMPAC package.[23] All calculations were made with a Silicon Graphics Indigo XZ workstation.

Theory

The topological properties of a scalar field such as $\varrho(r)$ and $-\nabla^2\varrho(r)$ are summarized in terms of their critical points, r_c, i.e. the points where $\nabla\varrho(r)$ and $\nabla(-\nabla^2\varrho(r))$ are equal to zero.[12] Critical points are classified according to their type (m,n) by stating their rank m and signature n. The rank is equal to the number of nonzero eigenvalues of the Hessian matrix of $\varrho(r)$ or $-\nabla^2\varrho(r)$ at r_c while the signature is the algebraic sum of the signs of the eigenvalues of ϱ or $-\nabla^2\varrho$. The interaction of two atoms leads to the formation of a (3, −1) critical point in $\varrho(r)$. The gradient paths which originate and terminate at this point define the bond path and the interaction surface that defines the atomic basins.[12] Along the bond path, $\varrho(r)$ has a minimum at r_c while it has maxima in the two directions that are perpendicular to the bond. The negative curvatures λ_i of $\varrho(r)$ at r_c measure the degree of contraction of the charge density perpendicular to the bond path while the positive one measures the degree of contraction toward each of the neighboring nuclei and away from the critical point. The nature of the bond formed will be reflected in the competition between these two types of charge density contractions. For ionic bonds, the positive curvature is much larger than the sum of the negative ones so that a relative depletion of charge exists around r_c.[12b] As a result of this, $-\nabla^2\varrho(r_c)$ is negative and $\varrho(r_c)$ is quite small.

(21) Frisch, M. J.; Trucks, G. W.; Head-Gordon, M.; Gill, P. M. W.; Wong, M. W.; Foresman, J. B.; Johnson, B. G.; Schlegel, H. B.; Robb, M. A.; Replogle, E. S.; Gomperts, R.; Andres, J. L.; Raghavachari, K.; Binkley, J. S.; Gonzalez, C.; Martin, R. L.; Fox, D. J.; Defrees, D. J.; Baker, J.; Steward, J. J. P.; Pople, J. A. *Gaussian 92*, Revision C; Gaussian Inc.: Pittsburgh, PA, 1992.

(22) Colbourn, E. A. *Surf. Sci. Rep.* **1992**, *15*, 281−319.

(23) Bader, R. F. W. Private communication, 1993.

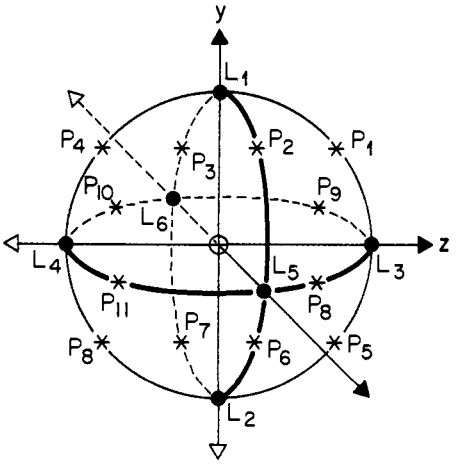

Figure 2. Atomic graph of $-\nabla^2\varrho(r)$ for the O^{2-} site in bulk MgO. The points denoted by L_i, with $i = 1-6$, indicate the location of the (3, −3), while the P_i points, with $i = 1-12$, show the position of the (3, −1) critical points.

Table 1. Values of the Charge Density $\varrho(r)$, of its Curvatures λ_i with $i = 1$, 2, and 3, and of $-\nabla^2\varrho(r)$ at the Mg−O Bond Critical Points Obtained for the Different Models

MgO	$\varrho(r_c)$ (au)	λ_1 (au)	λ_2 (au)	λ_3 (au)	$-\nabla^2\varrho(r$ (au)
bulk	0.035	−0.047	−0.047	0.354	−0.25
three layers	0.035	−0.047	−0.047	0.354	−0.25
two layers	0.033	−0.058	−0.058	0.470	−0.35
isolated Mg_5O_5 O(1)−Mg(2)	0.030	−0.040	−0.040	0.345	−0.26
isolated Mg_5O_5 O(1)−Mg(3)	0.038	−0.050	−0.048	0.347	−0.25
isolated Mg_5O_5 O(4)−Mg(3)	0.052	−0.064	−0.063	0.316	−0.18
emb Mg_5O_5 O(1)−Mg(2)	0.035	−0.049	−0.049	0.356	−0.25
emb Mg_5O_5 O(1)−Mg(3)	0.035	−0.049	−0.049	0.356	−0.25
emb Mg_5O_5 O(4)−Mg(3)	0.034	−0.047	−0.047	0.354	−0.26

The $-\nabla^2\varrho(r)$ distribution of a light atom reflects the quantum shell structure by exhibiting the corresponding number of alternating pairs of shells of charge concentration and depletion.[12] The outer (valence) shell of charge concentration contains a spherical surface over which $\varrho(r)$ is maximally concentrated. The distribution of $\varrho(r)$ over this surface in the free atom is uniform if one assumes that the nucleus has a negligible electric quadrupole moment. The formation of bonds produces changes in this distribution, and a number of local maxima, minima, and saddle points appear in this surface of charge distribution.[12] Their number, type, location, and $-\nabla^2\varrho(r)$ value are a function of the linked atoms.

In general, the type and number of critical points of $-\nabla^2\varrho(r)$ in the valence shell of a bonded atom are succinctly summarized by its atomic graph.[12a] This graph provides the connectivity of the extremes of the $-\nabla^2\varrho(r)$ in the corresponding valence shell distribution and may be seen in Figure 2 for the O^{2-} ion present in bulk MgO. In the Bader and co-workers' theory, the atomic graph also summarizes the information about the chemical reactivity of an atom in a molecule.[12e] The atomic reactivity is determined by the type and number of critical points found in its valence shell. For example, in a Lewis acid−base reaction, the largest local maximum corresponding to a (3, +3) critical point of the $-\nabla^2\varrho(r)$ distribution of the base reacts with the deepest available minimum characterized by a (3, +1) point in the acid molecule.[12e]

Results and Discussion

In order to obtain information about the charge distribution of the O^{2-} ion in the bulk, a calculation of bulk MgO was performed with the CRYSTAL program using the existing structural data. The results of the topological analysis of $\varrho(r)$ of the Mg−O bonds are shown in Table 1. The regions between the Mg and O nuclei in bulk MgO showed a low electronic concentration of $\varrho(r_c) = 0.035$ au and a negative value for the $-\nabla^2\varrho(r_c)$ that corresponds to a highly ionic bond between these

Table 2. Positions of the Critical Points and Values of $-\nabla^2\varrho(r)$ of the Valence Shell for the Different O Sites in Bulk MgO and in the MgO Layer Models

	critical point	r (au)	$-\nabla^2\varrho(r)$ (au)
bulk	$(3,-3)_i$	0.685	3.000
	$(3,+1)$	0.686	2.998
three layers surf sites	$(3,-3)_e$	0.682	3.142
	$(3,-3)_i$	0.684	3.055
	$(3,+1)$	0.687	2.921
inner sites	$(3,-3)$	0.685	3.002
	$(3,+1)$	0.686	2.995
two layers surf sites	$(3,-3)_e$	0.682	3.141
	$(3,-3)_i$	0.684	3.053
	$(3,+1)$	0.687	2.923
one layer surf sites	$(3,-3)$	0.681	3.191
	$(3,+1)$	0.681	2.854

atoms (closed-shell-type interaction).[11b] The value of $\varrho(r_c)$ is very close to that found NaCl,[11a] confirming the highly ionic nature of the MgO crystal. The large value of the positive curvature of $\varrho(r_c)$ showed that the electronic charge is concentrated away from the Mg−O bond critical point and into the anion atomic basins. The values of $\varrho(r_c)$ and $-\nabla^2\varrho(r_c)$ obtained for these bonds in the isolated clusters differ considerably from those obtained from the bulk and the two- and three-layer calculations. These differences are drastically reduced when charge embedding is employed in the clusters. In this case, the values of $\varrho(r_c)$ are very close to those obtained from the bulk and the slab calculations. This result shows that the field generated by the rest of the crystal noticeably modifies the charge distribution within each of the Mg−O bonds when the crystal is formed.

The atomic graph is very useful as its provides the connectivity of the extremes of the $-\nabla^2\varrho(r)$ in each valence shell. The graph of the O^{2-} ion in bulk MgO, shown in Figure 2, contains six critical points of the (3, −3) type, each located along a Mg−O bond direction, plus twelve (3, −1) points forming a tetragonal bipyramid and eight (3, +1) points located in the center of the faces of this figure. As seen in Table 2, the very small differences found between the values of $-\nabla^2\varrho(r)$ at the different critical points showed that the charge distribution of the O ion in the bulk presents only small departures from the spherical shape. This indicates that the charge distribution of the O is quite close to the classical model of a spherical ion in a highly ionic cubic crystal.[24]

In the three-layer calculation, the atomic graph of the O^{2-} ion in the surface contained two (3, −3) critical points located along the Mg−O bond direction, which is perpendicular to the MgO (001) surface as shown in Figure 3. In this graph, there are also four (3, −1) saddle points that are located along the Mg−O directions and four additional (3, +1) points located at the midpoints between these directions. The atomic graph of the O^{2-} located within the slab showed the same set of critical points for the $-\nabla^2\varrho(r)$ distribution as was found for bulk MgO. The results of the topological analysis of the $-\nabla^2\varrho(r)$ distribution are shown in Table 2. The values of the Laplacian of $\varrho(r)$ for the (3, −3) points of the O ions obtained for the bulk and for the center layer were the same, indicating that the slab calculation also provides a good approximation to the O charge density in the bulk.[18] For MgO slabs containing one and two layers, the atomic graph of the O^{2-} ions located in the surface was the same as in the three-layer case. The results of the topological analysis of the $-\nabla^2\varrho(r)$ distribution for this case are shown also in Table 2. The differences between the values of $-\nabla^2\varrho(r)$ for the (3, −3) points of the O ions at the surface

(24) Bloss, F. D. *Crystallography and Crystal Chemistry*; Holt, Rinehart & Winston: New York, 1971.

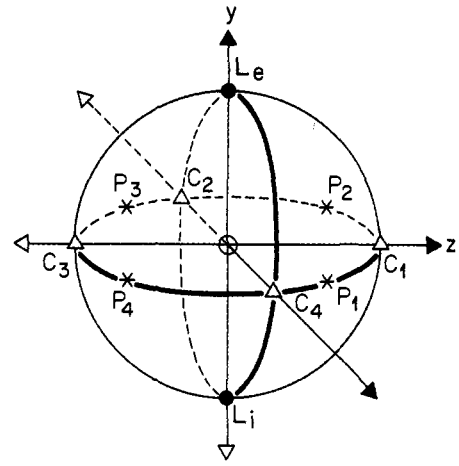

Figure 3. Atomic graph of $-\nabla^2\varrho(r)$ for the O^{2-} site in the MgO (001) surface. The L_e and L_i points indicate the location of the (3, −3) extremes along one of the O−Mg directions; the L_e point is located in the external side of the surface while L_i is in the internal one. The P_i points, with $i = 1-4$, show the positions of the (3, −1), and the C_i points, also with $i = 1-4$, those of the (3, +1) critical points.

Table 3. Positions of the Critical Points and Values of $-\nabla^2\varrho(r)$ of the Valence Shell for the Different O^{2-} Sites in the MgO Layer Models and in the Isolated and Embedded Cluster of MgO

	L_e (3, −3)		L_i (3, −3)		C (3, +1)	
	r (au)	$-\nabla^2\varrho(r)$ (au)	r (au)	$-\nabla^2\varrho(r)$ (au)	r (au)	$-\nabla^2\varrho(r)$ (au)
one layer	0.681	3.191	0.681	3.191	0.681	2.854
two layers	0.682	3.141	0.684	3.053	0.687	2.923
three layers	0.682	3.142	0.684	3.055	0.687	2.921
isolated Mg_5O_5	0.691	2.799	0.659	4.445	0.694	2.587
emb Mg_5O_5	0.680	3.146	0.684	3.091	0.688	2.873

are less than 2% for the different slab calculations. This result again shows the rapid convergence of the surface properties with the number of layers employed in the calculation.[19]

In order to validate the results obtained with the embedded cluster method, it is necessary to compare its values of $-\nabla^2\varrho(r)$ with those found for the slabs of MgO with the CRYSTAL program. This is a critcal comparison because the values of $-\nabla^2\varrho(r)$ are very sensitive to even minute variations of $\varrho(r)$.[12a] From Table 3, we see that the *ab-initio* calculation using the embedded cluster reproduces the values of $-\nabla^2\varrho(r)$ at critical points of the O ion found with CRYSTAL within less than 2%. This result indicates that the embedded cluster provides a reliable charge distribution for this ion in solid MgO. From Table 3, we see that the embedding of the MgO cluster has a remarkable influence over the values of $-\nabla^2\varrho(r)$ at the critical points of the O ion. If no embedding is used, large discrepancies (up to 33%) are found between the results obtained with GAUSSIAN and those derived with the CRYSTAL program. This result shows that the polarization generated by the rest of the crystal plays an important role in the final charge distribution of the O ions in MgO.

According to the theory of Bader and co-workers,[12a] the active sites in a molecule (or, as assumed in the present case, in an atomic surface) are associated with critical points of the $-\nabla^2\varrho(r)$ distribution of the valence shells. The available experimental information and the results obtained for the isolated MgO molecule[15] suggest that one may take the (3, +1) critical point of $-\nabla^2\varrho(r)$ of the O^- valence shell pointing outside the surface as the active site for the H abstraction. In this type of process, it was shown[15] that an electronically rich C−H fragment of the CH_4 molecule with a (3, −3) critical point will be directed toward the zone of the smallest charge concentration in the O^-

valence shell, which is a (3, +1) point in the MgO molecule. The atomic graph of the O^{2-} ion in the surface of pure MgO shows instead a (3, −3) critical point for $-\nabla^2\varrho(r)$ distribution that corresponds to a local maximum in a direction perpendicular to the (001) surface. This shows that a perfect MgO surface does not have O sites with regions of charge depletion that are required for the H abstraction of methane (or, for similar reasons, of other hydrocarbons and of H_2). This lack of reactivity of the O^{2-} site is not so surprising because this ion is isoelectronic with the Ne atom. This type of electronic distribution is well-known for its low chemical reactivity.[12a] In their *ab-initio* work, Børve and Pettersson[10a] found that the O^{2-} site in MgO does not associate with the methyl radical in the MgO (001) surface because a net repulsive interaction exists between them. This result lends additional support to the conclusion regarding the lack of reactivity of the O^{2-} site in a (001) MgO surface toward the H abstraction.

It is interesting to point out that the O^- ion has an electronic configuration similar to that of the highly reactive atomic F.[12] Then, at first sight, one should expect a highly reactive O site every time that this electronic structure is stabilized in a surface. Nevertheless, as found in the MgO and LiO molecules,[15] the existence of a O^- ion is a necessary but not a sufficient condition for high chemical reactivity. The reason for this is that an ion with a given total charge may have quite different topologies depending on the field acting on it.[15] Only a few of these charge distributions of the O ion will have the characteristics that will render them highly reactive. It is then important to study the topology of $-\nabla^2\varrho(r)$ of the MgO surface and its relationship with the chemical reactivity of the different O sites. The value of $-\nabla^2\varrho(r)$ at the (3, +1) critical point of the active site was found to predict the relative reactivity in nucleophilic additions.[12c,d] The lower the value of the $-\nabla^2\varrho(r)$ at this point, the higher the reactivity of the site toward nucleophilic additions. Such a trend was also observed for the H abstraction from methane, considering as active sites the outer (3, +1) saddle points in the O^- valence shell of the MgO and LiO molecules.[15] This trend reflects the fact that the electron-rich C−H fragment of methane will react more readily with the O sites that have the lower charge concentration in their (3, +1) point of their valence shell. In Figure 4 are shown the effects of a Mg^+ vacancy and of doping ions such as Li^+ on the topology of the valence shell of the O ion at the (001) surface of MgO. In the case of doping in the second layer below the O site, its (3, −3) critical point of $-\nabla^2\varrho(r)$ that is located in a direction perpendicular to this surface is changed into a saddle point of the (3, +1) type. This change shows that the local maximum of $-\nabla^2\varrho(r)$ of the O^{2-} ion has been converted into a local minimum in the O^- site by the doping. As found experimentally,[1-4] the catalytic activity in MgO increases with doping in such a way that it is the largest for Li and decreases for Na and for K. This trend correlates well with the changes found in the values of $-\nabla^2\varrho(r)$ at the (3, +1) local minimum of the surface O^- ion in the different MgO clusters (see Table 4). The deepest local minimum of the O valence shell is found in the MgO cluster doped with Li while, for the other dopants, the minimum decreases according to the diminishing H abstraction power of the dopant (Li > Na > K). This trend suggests that a correlation exists between the depth of the minimum at the valence shell and the H-abstracting power of an O^- site in the (001) surface of MgO.

As the Madelung potential plays an important role in the charge distribution of the O sites in MgO,[22] it is likely that the O sites in the surface of other atomic planes will have local minima of different depths and, therefore, show variations in their H-abstraction power and chemical reactivity. This also

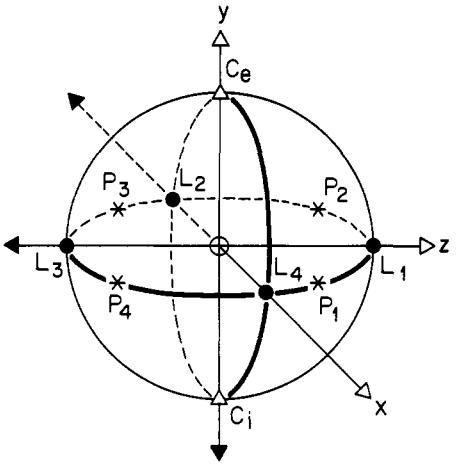

Figure 4. Atomic graph of $-\nabla^2\varrho(r)$ for the O^- active site in the doped MgO (001) surface. C_e and C_i indicate the locations of the (3, +1) points along the O−X direction, with X = Li, Na, and K; the C_e point is located in the external side of the surface while C_i is in the internal one. The P_i points, with $i = 1-4$, show the positions of the (3, −1), and the L_i points, with $i = 1-4$, those of the (3, −3) critical points. The same atomic graph was found for the O^- ion when a Mg^+ vacancy was introduced in the second layer of the MgO cluster (M_2 site of Figure 1).

Table 4. Positions of the Critical Points and Values of $-\nabla^2\varrho(r)$ of the Valence Shell for the Different O^- Sites in a MgO Cluster Doped with Li, Na, and K and in One with a Mg^+ Vacancy ([Va] Represents a Mg^+ Vacancy)

	L		C_e		C_i	
	r (au)	$-\nabla^2\varrho(r)$ (au)	r (au)	$-\nabla^2\varrho(r)$ (au)	r (au)	$-\nabla^2\varrho(r)$ (au)
Mg_4LiO_5	0.659	4.773	0.733	0.497	0.730	0.510
Mg_4NaO_5	0.659	4.742	0.732	0.538	0.729	0.522
Mg_4KO_5	0.659	4.712	0.730	0.580	0.727	0.551
$Mg_4[Va]O_5$	0.660	4.763	0.730	0.628	0.725	0.575

indicates that, in real MgO surfaces, where quite different atomic planes may be present,[22] a wide distribution of O sites and consequently of chemical reactivity occurs.

The conclusions reached for methane regarding the H-abstracting power of the O^- ion of the surface of the doped MgO are likely to be valid for other electron-rich H−C bonds of more complex hydrocarbons as long as the bond charge distribution is more or less similar to that of methane. The extension to other compounds containing an H−X bond depends on the electronegativity of X because this atom may deplete the charge distribution of the H in such a way that it loses its "basic" character. As a result of this loss, the gain in the potential energy density resulting from the filling of the hole in one charge density is not realized[12a] and other reaction paths may become more likely.

The remaining critical points of $-\nabla^2\varrho(r)$ of the atom graph of the O^- ion of the doped MgO cluster are four (3, −3) local maxima located in the plane of the (001) surface at the midpoints between the Mg−O bond directions. Additionally, four (3, −1) points are located along the Mg−O directions (see Figure 4). In the bulk O^{2-} ions, as already mentioned, the atomic graph is more complex and contains six critical points of the (3, −3) type, each located along a Mg−O bond direction, plus twelve (3, −1) points forming a tetragonal bipyramid and eight (3, +1) points located at the center of each face. The change from an O^{2-} to an O^- ion produced a drastic modification in both the nature and the number of the critical points of $-\nabla^2\varrho(r)$. A Mg^+ vacancy or the substitution of a Mg^{2+} ion by a Li^+, a Na^+, or a K^+ ion in the second layer produces a significant rearrange-

ment of the charge distribution of the O ion located in the surface above it. When two ions of different charge interact, both the anion and cation must be polarized in a direction counter to that of the charge transfer in order to achieve electrostatic equilibrium.[12a] The cationic nucleus is attracted by the charge of the anion, and the electron density of the cation must polarize away from the anion to balance this force. The anionic nucleus is repelled by the positive charge of the cation, and its electron density must move toward the cation to balance this repulsion. The complex changes found in the O ions in the surface of MgO upon doping or vacancy formation are a result of two different contributions: (a) a variation in the degree of charge transfer to the O atom and (b) a change in its shell polarization as fewer Mg^{2+} ions are interacting with this particular O ion. The substitution of a Mg^{2+} ion in the second layer by a single charged ion or vacancy produces a decrease in the amount of electron density present in the O ion of the surface. For this ion of the doped MgO, the field of only the neighboring Mg^{2+} ions in the surface is able to convert the O saddle points found in the bulk in this plane into (3, −3) points of $-\nabla^2\varrho(r)$ distribution. The single charged ion or vacancy seems to be unable to compete with the field of the Mg^{2+} ions, so the local maxima found in the bulk along the Mg−O direction perpendicular to the surface are now converted into (3, +1) saddle points with much lower charge concentrations that favor the H abstraction.

Conclusions

We conclude that (a) $-\nabla^2\varrho(r)$ can be employed in the evaluation of the chemical reactivity of model active sites in the H abstraction from CH_4 by pure and doped solid MgO, (b) the topology of $-\nabla^2\varrho(r)$ associated with the reactivity of active sites predicts the correct trend found in doped MgO for the H abstraction, and (c) the results obtained suggest that, in order to improve the activity of MgO toward H abstraction from methane or similar hydrocarbons, one has to choose the doping metal that produces the lowest charge concentration at the saddle point in the O^- valence shell and/or increase the number of vacancies in the second layer of the (001) face of the MgO crystal.

Acknowledgment. The authors want to acknowledge CONICIT of Venezuela (Project PI-092) for providing funding for the Silicon Graphics Indigo workstation used in this work, to Dr. Carlo Gatti from the Centro CNR (S.R.S.R.C., Milano, Italy, for useful discussions and for lending some of his programs used in determining critical points, and to Dr. J. Rivero Charlton for his valuable help in computational and linguistic matters.